

Validity test of the Trojan Horse Method applied to the ${}^7\text{Li} + \text{p} \rightarrow \alpha + \alpha$ reaction via the ${}^3\text{He}$ break-up

A. Tumino^{1,2,a}, C. Spitaleri^{1,2}, M.L. Sergi^{1,2}, V. Kroha³, V. Burjan³, S. Cherubini^{1,2}, Zs. Fülöp⁴, M. La Cognata^{1,2}, L. Lamia^{1,2}, J. Novák³, R.G. Pizzone², S. Romano^{1,2}, E. Somorjai⁴, S. Tudisco^{1,2}, and J. Vincour³

¹ Dipartimento di Metodologie Fisiche e Chimiche per l'Ingegneria, Università di Catania, Catania, Italy

² INFN Laboratori Nazionali del Sud, Catania, Italy

³ Nuclear Physics Institute of ASCR, Rez near Prague, Czech Republic

⁴ Institute of Nuclear Research of Hungarian Academy of Sciences (ATOMKI), Debrecen, Hungary

Received: 20 June 2005 /

Published online: 10 March 2006 – © Società Italiana di Fisica / Springer-Verlag 2006

Abstract. The Trojan Horse Method (THM) was applied to the ${}^3\text{He}+{}^7\text{Li}$ interaction in order to investigate the quasi-free ${}^7\text{Li}(\text{p},\alpha){}^4\text{He}$ reaction. The three-body experiment was performed at 33 MeV corresponding to a ${}^7\text{Li}$ -p relative energy ranging from 50 keV to 7 MeV. The extracted ${}^7\text{Li}(\text{p},\alpha){}^4\text{He}$ quasi-free cross-section was compared with the behavior of direct data, as well as with the result of a previous THM investigation on the ${}^7\text{Li}(\text{p},\alpha){}^4\text{He}$ reaction off the neutron in ${}^2\text{H}$. A good agreement between data sets shows up throughout the energy range investigated, providing a very important validity test of the pole approximation for the THM.

PACS. 24.10.-i Nuclear-reaction models and methods – 25.40.-h Nucleon-induced reactions

1 Introduction

In the last years, the Trojan Horse Method (THM) [1, 2, 3, 4, 5, 6, 7, 8, 9, 10, 11, 12] has proven to be a successful indirect approach for studying charged-particle two-body reactions relevant for astrophysics. The Trojan Horse Method selects the quasi-free contribution of an appropriate three-body $A + a \rightarrow c + C + s$ reaction performed at energies well above the Coulomb barrier to extract the relevant two-body $A + x \rightarrow c + C$ reaction cross-section at astrophysical energies free of Coulomb suppression as well as electron screening effects. The method is based on previous studies on quasi-free (QF) scattering and reactions [13, 14, 15, 16, 17], where evidence for a QF mechanism at energies of few tens of MeV was observed and justified by the high momentum transferred to the outgoing particles, due to the high Q -value of the reactions involved. When applying the method, kinematical conditions are appropriately chosen in order that s be spectator to the process and the x - s binding energy “enough” to compensate for the $A+a$ relative motion. The prescription to calculate the accessible astrophysical energy region is given by

$$\Delta E_{qf} = E_{Ax} - B_{xs} \pm E_{xs}, \quad (1)$$

where E_{Ax} is the beam energy in the center of mass of the two-body A - x system, B_{xs} represents the binding energy

for the x - b system and E_{xs} describes their inter-cluster motion within a chosen cutoff in momentum. A key role is thus played by the “Trojan Horse nucleus” a , whose wave function is required to have a large amplitude for a $x - s$ cluster configuration. However, a general view of the influence of its bound structure on the validity of the pole approximation for the THM is still missing. Recently this problem was addressed within an experimental program to indirectly study relevant reactions destroying Li isotopes in stellar environments. In particular the ${}^7\text{Li}(\text{p},\alpha){}^4\text{He}$ reaction, key reaction in the so-called “Li problem”, was first investigated via ${}^2\text{H}$ break-up and then by picking the proton up from ${}^3\text{He}$. From the first investigation via the ${}^2\text{H}({}^7\text{Li},\alpha\alpha)\text{n}$ break-up process, very interesting results were obtained [3, 6, 7, 18]. Two resonances, associated with the group of ${}^8\text{Be}$ states between 19.9 and 20.2 MeV and that around 22.2 MeV of excitation energy, contributing to the ${}^7\text{Li}$ -p direct cross section, could be observed also in the indirect ${}^7\text{Li}$ -p excitation function [18]. Moreover, the behavior of the THM $S(E)$ -factor at low energy was found to be in very good agreement with that of standard measurements in the region where screening effects are negligible. Estimates of the bare nucleus S_0 factor and electron screening potential U_e were obtained in PWIA [6] as well as applying the more sophisticated MPWBA [5, 7], confirming the values from direct measurement, but with smaller errors. Direct values are indeed affected by larger

^a e-mail: tumino@lns.infn.it

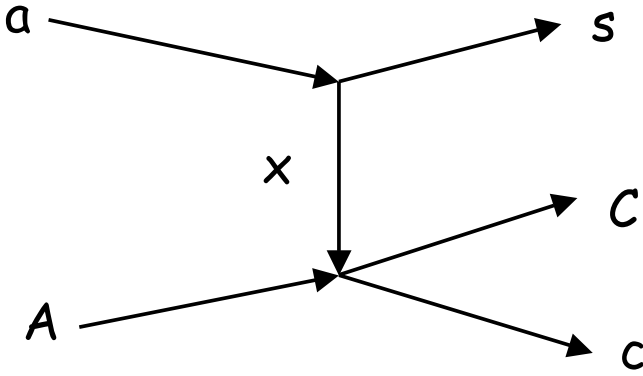


Fig. 1. Diagram representing the quasi-free $A+a \rightarrow c+C+s$ reaction; the nucleus A interacts only with the cluster x , leaving particle s as spectator to the process.

uncertainties due to the extrapolation procedure employed to get them [19]. In the present paper the THM results of the ${}^7\text{Li}(p, \alpha){}^4\text{He}$ reaction via the ${}^7\text{Li}({}^3\text{He}, \alpha\alpha){}^2\text{H}$ three-body experiment analysed in PWIA are presented. A ${}^7\text{Li}$ - p relative energy range (0.2–7 MeV) including the mentioned resonances, was populated. Results may be eventually different due to the presence of a different “Trojan Horse nucleus” (${}^3\text{He}$ instead of ${}^2\text{H}$). Moreover a charged spectator, as in the present case, may introduce some distortions in the exit channel. A good agreement between direct and indirect two-body excitation functions also in this case, would provide a very important validity test of the pole approximation as well as of invariance of the reaction amplitude for the two-body channel.

2 Plane-Wave Impulse Approximation

In the phase space region where the QF mechanism is expected to be present, the Impulse Approximation [20, 21] can be applied, which describes the quasi free $A+a \rightarrow c+C+s$ reaction by a Pseudo Feynman diagram (see fig. 1).

A pole of the diagram refers to the break-up of the target nucleus a into the clusters x and s , and the other one contains the information on the virtual $A+x \rightarrow c+C$ two-body process. In order that this description be valid, the following conditions have to be fulfilled [20]:

- The momentum transfer sufficiently high or equivalently the associated wavelength sufficiently smaller (less than 1 fm). Consequently the $A-x$ interaction can be considered confined.
- The incident center-of-mass energy higher than the binding energy of clusters x - s .

In the Plane-Wave Impulse Approximation (PWIA) the cross section of the three-body reaction can be factorized into two terms corresponding to the two poles of fig. 1 [22, 23] and it is given by

$$\frac{d^3\sigma}{dE_c d\Omega_c d\Omega_C} \propto KF \left(\frac{d\sigma}{d\Omega_{cm}} \right)^{off} \cdot |\Phi(\mathbf{p}_s)|^2, \quad (2)$$

where

- $[(d\sigma/d\Omega)_{cm}]^{off}$ is the off-energy-shell differential cross section for the two body $A(x, c)C$ reaction at the center-of-mass energy E_{cm} given in post collision prescription by

$$E_{cm} = E_{c-C} - Q_{2b}, \quad (3)$$

where Q_{2b} is the two body Q -value of the $A+x \rightarrow c+C$ reaction and E_{c-C} is the relative energy between the outgoing particles c and C .

- KF is a kinematical factor containing the final-state phase-space factor and it is a function of masses, momenta and angles of the outgoing particles:

$$KF = \frac{\mu_{Aa} m_c}{(2\pi)^5 \hbar^7} \frac{p_C p_c^3}{p_{Aa}} \left[\left(\frac{p_{Bx}}{\mu_{Bx}} - \frac{p_{Cc}}{m_c} \right) \cdot \frac{p_c}{p_c} \right]^{-1}. \quad (4)$$

- $\Phi(\mathbf{p}_s)$ is the momentum distribution of the spectator particle. In PWIA it is given by the Fourier transform of the radial wave function $\chi(\mathbf{r})$ for the x - s inter-cluster motion, usually described in terms of Hankel, Eckart and Hulthen functions depending on the x - s system properties. Within momentum values of 40–50 MeV/ c , its shape cannot be distinguished by those ones associated with more sophisticated approaches.

In the experimental work reported in the present paper, the validity conditions of the IA appear to be fulfilled. Indeed ${}^3\text{He}$ has a quite high energy of 33 MeV (610 MeV/ c in momentum) corresponding to an associated de Broglie wavelength of 0.32 fm, much smaller than the ${}^3\text{He}$ mean square radius of 1.95 fm. Once measured the three-body cross-section, one can extract the cross-section for the $A+x$ interaction from eq. (2), under the assumption that off-energy-shell effects are negligible. However, this assumption has to be verified from comparison with direct data.

3 The experiment

The ${}^7\text{Li}({}^3\text{He}, \alpha\alpha){}^2\text{H}$ experiment was performed at the Nuclear Physics Institute of ASCR in Rez, near Prague. A 33 MeV ${}^3\text{He}$ cyclotron beam was delivered onto an isotopically enriched lithium fluoride target (${}^7\text{Li} \approx 95\%$). Two silicon ΔE - E telescopes for α 's identification, consisting of 20 μm ΔE - and 1000 μm position-sensitive E -detector, were placed on opposite sides with respect to the beam direction covering the laboratory angles 94.6° to 109.4° and 44.3° to 59.7°. The angular ranges were chosen in order to cover momentum values p_s of the undetected deuteron ranging from about –100 MeV/ c to about 100 MeV/ c . This assures that the bulk of the QF contributions for the break-up process of interest falls inside the investigated regions, allowing also to cross check the method outside the relevant phase-space regions. The trigger for the event acquisition was given by the coincidences between the two telescopes.

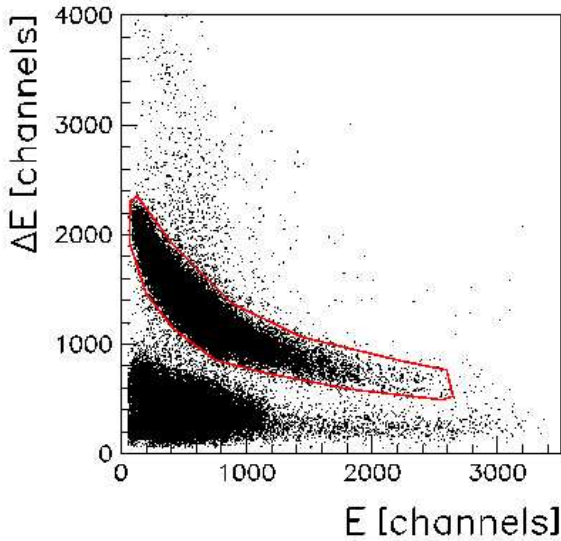


Fig. 2. Example of ΔE - E 2D-plot; the graphical cut to select the α -particles is shown as full line.

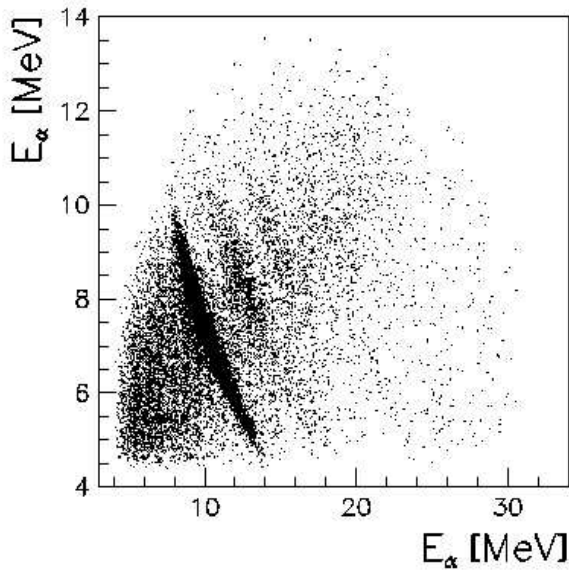


Fig. 3. Locus of events in the E_α vs. E_α plane. The correlated group of events corresponds to ${}^8\text{Be}$ excited states, feeding the two α 's in the exit channel.

4 Data analysis and results

The energy and position calibration of the telescopes was performed using data acquired in preliminary runs of the ${}^3\text{He} + {}^{197}\text{Au}$ elastic scattering. A standard three-peak α source was also used. In order to identify the channel of interest and to choose the kinematical conditions where the quasi-free process is dominant, α loci were selected in the ΔE - E two-dimensional plots. An example of the ΔE - E plot is shown in fig. 2, with the graphical cut to select the α -particles. The kinematics were reconstructed

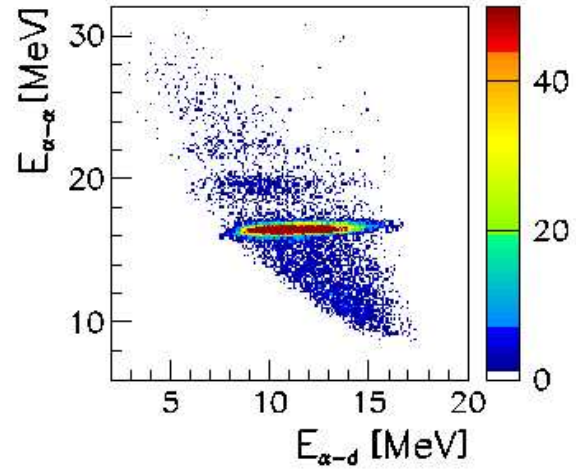


Fig. 4. Coincidence events in the α - α vs. α - d relative energy plane.

under the assumption of a deuteron as third particle, leading to the locus of events in the E_α vs. E_α plane shown in fig. 3. It reproduces very well the one calculated by using a three-body kinematical calculation. At least three correlated groups of events can be recognized in the figure, corresponding to excited states of ${}^8\text{Be}$, which decay into the two α 's in the exit channel. The first group from the left is fed by the 16.6 and 16.9 MeV states, the second one is due to the states between 19.9 and 20.2 MeV, while the third one corresponds to the 22.2 and 22.9 MeV levels. These states have all isospin $T = 0$ and natural parity. The Q -value spectrum for these events shows a peak at about 12 MeV, which refers to the $\alpha + \alpha + d$ channel of interest whose calculated Q -value is 11.85 MeV. However, the Q -value for the ${}^7\text{Li}(p, \alpha){}^4\text{He}$ two-body reaction (17.35 MeV) is larger than the excitation energies of the ${}^8\text{Be}$ states contributing to the first group of events. Thus these states will not appear as resonances in the ${}^7\text{Li}$ - p excitation function. The resulting spectra make us confident on the quality of the performed calibration, and on the possibility to well identify the $\alpha + \alpha + d$ channel. Another representation of the coincidence events is given by projecting them onto the 2D-plot of relative energies for any two of the three final particles. The 2D-plot for α - α vs. α - d relative energies is shown in fig. 4. In this representation very clear horizontal loci show up, corresponding to the groups of ${}^8\text{Be}$ states recognized in fig. 2. As expected, neither vertical nor diagonal loci associated with the excitation of ${}^6\text{Li}$, seem to be present, because no α decaying states can contribute in this α - d relative energy region.

The ${}^8\text{Be}$ excited states can be populated via quasi-free mechanism or via sequential decay. A way to investigate the reaction mechanism involved and to disentangle quasi-free coincidence events from other, is to investigate the behavior of the coincidence yield depending on the deuteron momentum p_s for all coincidence events, in the whole angular range covered by the detectors. Relative

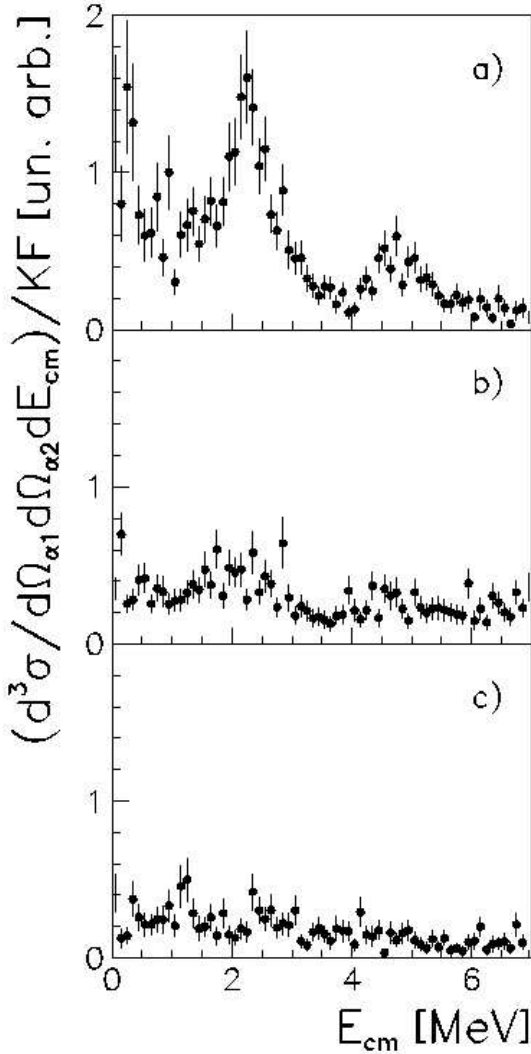


Fig. 5. Coincidence yield projected onto the ${}^7\text{Li-p}$ energy axis (E_{cm}) for different p_s ranges: $0 \text{ MeV}/c \leq |p_s| \leq 30 \text{ MeV}/c$ (a), $30 \text{ MeV}/c \leq |p_s| \leq 60 \text{ MeV}/c$ (b) and $|p_s| \geq 60 \text{ MeV}/c$ (c).

energy $E_{7\text{Li-p}}$ spectra ($E_{7\text{Li-p}}$ corresponds to the E_{cm} variable of eq. (2)) divided by the phase-space contribution were reconstructed for different ranges of the deuteron momentum p_s . Within $0 \text{ MeV}/c \leq |p_s| \leq 30 \text{ MeV}/c$ (fig. 5a) and $30 \text{ MeV}/c \leq |p_s| \leq 60 \text{ MeV}/c$ (fig. 5b) momentum ranges, the coincidence yield appears to be quite high in particular close to the $E_{7\text{Li-p}}$ resonant window. Moving a bit far in momentum ($|p_s| > 60 \text{ MeV}/c$), the coincidence yield drastically decreases as shown in fig. 5c.

A strong correlation between coincidence yield and deuteron momentum p_s shows up, a necessary condition for the dominance of the quasi-free mechanism in the region approaching zero deuteron momentum. But in case of resonances in the low p_s region, this result might be not a sufficient condition, since the correlation can be partially depending on the resonant behavior, regardless of its se-

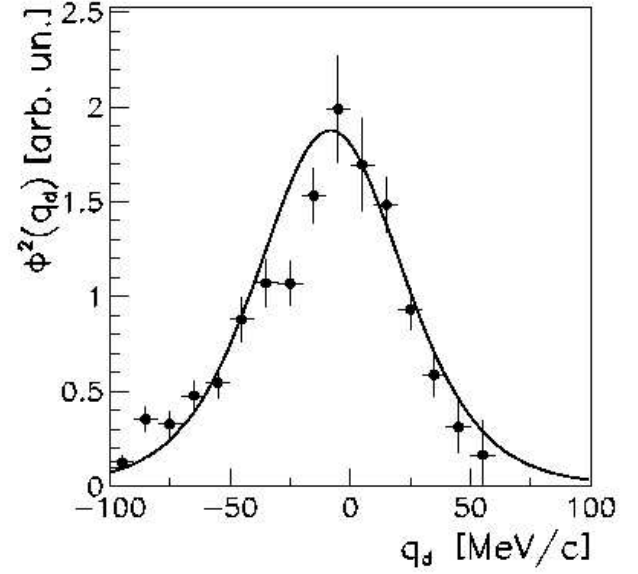


Fig. 6. Experimental deuteron momentum distribution. The full line represents the shape of the theoretical Hulthén function in momentum space.

quential decay- or quasi free-origin. An observable which turns out to be more sensitive to the reaction mechanism is the shape of the experimental momentum distribution for the deuteron. The experimental momentum distribution was reconstructed in Plane-Wave Impulse Approximation (PWIA) by applying the energy sharing method [24] to our coincidence data selecting ${}^7\text{Li-p}$ relative energy windows of 100 keV. The ${}^7\text{Li-p}$ relative energy was calculated in post collision prescription from eq. (3). Data were analyzed in PWIA, applying the factorization of eq. (2), and taking as $\Phi(\mathbf{p}_s)$ the Fourier transform of the radial wave function for the p-d intercluster motion inside ${}^3\text{He}$, described in terms of a Hulthén function

$$\Phi(\mathbf{r}) = \sqrt{\frac{ab(a+b)}{2\pi(a-b)^2}} \frac{1}{r} (e^{-ar} - e^{-br}) \quad (5)$$

with parameters $a = 0.2317 \text{ fm}^{-1}$ and $b = 1.202 \text{ fm}^{-1}$ [18]. Dividing the three-body coincidence yield by the kinematical factor, we are left with a quantity proportional to the product of the momentum distribution with the differential ${}^7\text{Li-p}$ two-body cross-section. Since in the restricted relative energy ranges of 100 keV, the differential two-body cross-section can be considered constant, the quantity above reflects the behavior of the experimental momentum distribution in arbitrary units. The result is reported in fig. 6. The full line superimposed onto the data represents the shape of the theoretical Hulthén function, which is normalized to the experimental maximum. A quite good agreement shows up, making us confident that in the experimentally selected kinematical region, the quasi-free mechanism gives the main contribution to the ${}^3\text{He} + {}^7\text{Li}$ reaction and it can be selected without

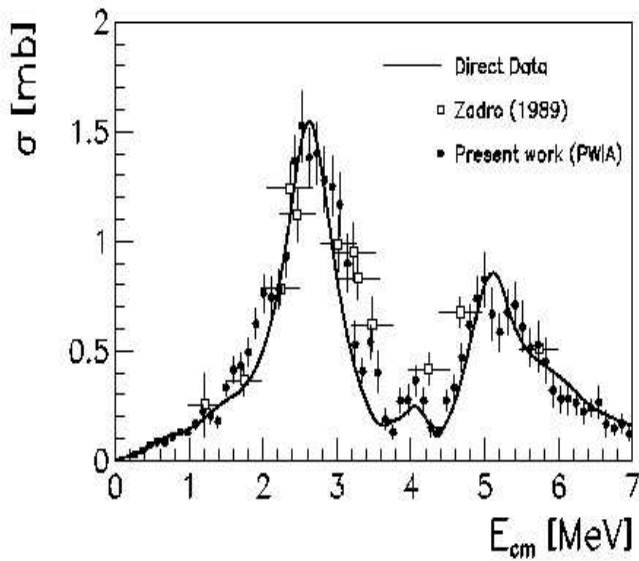


Fig. 7. Quasi-free data from the present experiment (full dots), direct cross-section (full line) from [19,26,27] and previous quasi-free data from ${}^2\text{H}$ break-up (open squares) [18].

significant interference with contaminant sequential decay processes. The further analysis was performed by considering coincidence events with a neutron momentum ranging between -30 and 30 MeV/ c . Following the PWIA approach, the two-body cross-section was derived dividing the selected three-body coincidence yield by the result of a Monte Carlo calculation reproducing the behavior of the $KF\Phi(\mathbf{p}_s)$ product (see eq. (2)). The geometrical efficiency of the experimental setup as well as the detection thresholds were accounted for in the calculation. An error calculation for the ${}^7\text{Li}$ - p relative energy was also performed giving a value ranging from 80 to 120 keV, the minimum estimate corresponding to the phase space region where the lens effect is more efficient [25]. In the extracted off-energy shell ${}^7\text{Li}$ - p two-body cross-section, penetrability effects were included before the comparison with direct data [19,26,27]. Both s and p waves in the entrance channel had to be considered, the s -wave describing the non-resonant behavior, while the p -wave being responsible of the resonant contributions. Thus Coulomb as well as $l = 1$ centrifugal barrier were accounted for in the procedure. In order to perform the comparison, direct data were integrated over the same θ_{cm} angular region covered in the present experiment (50° – 70°), θ_{cm} , being the emission angle for one outgoing α -particle in the α - α center-of-mass system [4,7,8,11]. The comparison is shown in fig. 7, where full dots represent our data, while the behavior of direct data from [19,26,27] is shown as full line, both sets averaged out at the same energy bin of 100 keV comparable with the uncertainty. The normalization to the direct data was performed in the ${}^7\text{Li}$ - p relative energy region between 2 and 3 MeV. Our former data via ${}^2\text{H}$ break-up [18] are

also reported in the figure as open squares. Data sets agree quite well throughout the investigated range, including the resonant regions. It is important to underline that with a single normalization parameter it was possible to reproduce the direct cross section over a wide ${}^7\text{Li}$ - p relative energy range. The good agreement validates the pole approximation for this experiment together with the PWIA approach and, importantly, the present results with ${}^3\text{He}$ as “Trojan Horse nucleus” agree with the previous investigation of the ${}^7\text{Li}(p, \alpha){}^4\text{He}$ reaction off the neutron in ${}^2\text{H}$. Therefore the invariance of the reaction amplitude for this two-body process is confirmed within the experimental errors.

5 Conclusions

The ${}^7\text{Li}(p, \alpha){}^4\text{He}$ reaction was investigated by selecting the quasi-free contribution to the ${}^3\text{He}({}^7\text{Li}, \alpha\alpha){}^2\text{H}$ three-body reaction performed at 33 MeV. The two-body cross-section was deduced in PWIA approach and compared with the direct behavior as well as with previous indirect data from the ${}^7\text{Li}(d, \alpha\alpha)n$ [18]. The good agreement between the sets of data suggests that ${}^3\text{He}$ is a good “Trojan Horse nucleus”, in spite of its quite high binding energy (5.85 MeV) and that the validity of the pole approximation, at least for the ${}^7\text{Li}+p$ interaction, is not “Trojan Horse nucleus” dependent. Although the present analysis in PWIA does not include Coulomb distortions due to the charged spectator, these effects seem not so important. The possibility to employ the simple PWIA is a relevant result, because it allows to simplify the theoretical formulation. However, from recent THM investigations [7,11,12] it comes out that more sophisticated approaches can be needed at sub-Coulomb energies in order to extract the cross-section of astrophysical interest. An important effect to be considered is the Coulomb distortion in the particle wave functions of the two-body exit channel. Further investigation of this experimental work with theoretical approaches based on the DWBA formalism is thus needed in order to better understand these important aspects.

This work was supported in part by OTKA T49245 and IN64269.

References

1. G. Baur, Phys. Lett. B **178**, 135 (1986).
2. S. Cherubini, V.N. Kondratyev, M. Lattuada, C. Spitaleri, Dj. Miljanić, M. Zadro, G. Baur, Astrophys. J. **457**, 855 (1996).
3. C. Spitaleri, M. Aliotta, S. Cherubini, M. Lattuada, Dj. Miljanić, S. Romano, N. Soić, M. Zadro, R.A. Zappalà, Phys. Rev. C **60**, 055802 (1999).
4. C. Spitaleri, M. Aliotta, P. Figuera, M. Lattuada, R.G. Pizzone, S. Romano, A. Tumino, C. Rolfs, L. Gialanella, F. Strieder, S. Cherubini, A. Musumarra, Dj. Miljanić, S. Typel, H.H. Wolter, Eur. Phys. J. A **7**, 181 (2000).
5. S. Typel, H. Wolter, Few-Body Syst. **29**, 7 (2000).

6. M. Aliotta, C. Spitaleri, M. Lattuada, A. Musumarra, R.G. Pizzone, A. Tumino, C. Rolfs, F. Strieder, *Eur. Phys. J. A* **9**, 435 (2000).
7. M. Lattuada, R.G. Pizzone, S. Typel, P. Figuera, Dj. Miljanić, A. Musumarra, M.G. Pellegriti, C. Rolfs, C. Spitaleri, H.H. Wolter, *Astrophys. J.* **562**, 1076 (2001).
8. C. Spitaleri, S. Typel, R.G. Pizzone, M. Aliotta, S. Blagus, M. Bogovac, S. Cherubini, P. Figuera, M. Lattuada, M. Milin, Dj. Miljanić, A. Musumarra, M.G. Pellegriti, D. Rendić, C. Rolfs, S. Romano, N. Soić, A. Tumino, H.H. Wolter, M. Zadro, *Phys. Rev. C* **63**, 005801 (2001).
9. A. Tumino, C. Spitaleri, S. Cherubini, A. Di Pietro, P. Figuera, M. Lattuada, A. Musumarra, M.G. Pellegriti, R.G. Pizzone, S. Romano, C. Rolfs, S. Tudisco, S. Typel, *Nucl. Phys. A* **718**, 499 (2003).
10. C. Spitaleri, S. Cherubini, A. Del Zoppo, A. Di Pietro, P. Figuera, M. Gulino, M. Lattuada, Dj. Miljanić, A. Musumarra, M.G. Pellegriti, R.G. Pizzone, C. Rolfs, S. Romano, S. Tudisco, A. Tumino, *Nucl. Phys. A* **719**, 99 (2003).
11. A. Tumino, C. Spitaleri, A. Di Pietro, P. Figuera, M. Lattuada, A. Musumarra, M.G. Pellegriti, R.G. Pizzone, S. Romano, C. Rolfs, S. Tudisco, S. Typel, *Phys. Rev. C* **67**, 065803 (2003).
12. C. Spitaleri, L. Lamia, A. Tumino, R.G. Pizzone, S. Cherubini, A. Del Zoppo, P. Figuera, M. La Cognata, A. Musumarra, M.G. Pellegriti, A. Rinollo, C. Rolfs, S. Romano, S. Tudisco, *Phys. Rev. C* **63**, 055806 (2004).
13. M. Jain, P.G. Roos, H.G. Pugh, H.D. Holgrem, *Nucl. Phys. A* **153**, 49 (1970).
14. J. Kasagi, T. Nakagawa, N. Serine, T. Tohei, H. Ueno, *Nucl. Phys. A* **239**, 233 (1975).
15. N. Arena, D. Vinciguerra, F. Riggi, C. Spitaleri, *Lett. Nuovo Cimento* **17**, 231 (1976).
16. M. Lattuada, F. Riggi, C. Spitaleri, D. Vinciguerra, *Phys. Rev. C* **26**, 1330 (1982).
17. S. Barbarino, M. Lattuada, F. Riggi, C. Spitaleri, D. Vinciguerra, *Phys. Rev. C* **21**, 1104 (1980).
18. M. Zadro, Dj. Miljanić, C. Spitaleri, G. Calvi, M. Lattuada, F. Riggi, *Phys. Rev. C* **40**, 181 (1989).
19. S. Engstler, G. Raimann, C. Angulo, U. Greife, C. Rolfs, U. Schröder, E. Somorjai, B. Kirch, K. Langanke, *Z. Phys. A* **342**, 471 (1992).
20. G.F. Chew, *Phys. Rev.* **80**, 196 (1950).
21. N.S. Chant, P.G. Roos, *Phys. Rev. C* **15**, 57 (1977).
22. U.G. Neudatchin, Y.F. Smirnov, *At. Energy Rev.*, **3**, 157 (1965).
23. G. Jacob, Th.A. Maris, *Rev. Mod. Phys.* **38**, 121 (1966).
24. N. Arena, D. Vinciguerra, F. Riggi, C. Spitaleri, *Nuovo Cimento* **45**, 405 (1978).
25. G. Baur, H. Rebel, *Annu. Rev. Nucl. Part. Sci.* **46**, 321 (1996).
26. G.S. Mani *et al.*, *Nucl. Phys.* **60**, 588 (1964).
27. Y. Cassagnou *et al.*, *Nucl. Phys.* **33**, 449 (1962).